Radio Science, Volume 22, Number 7, Pages 1261–1272, December 1987

Sheet simulation of a thin dielectric layer

Thomas B. A. Senior and John L. Volakis

Radiation Laboratory, Department of Electrical Engineering and Computer Science, University of Michigan, Ann Arbor

(Received October 27, 1986; revised April 13, 1987; accepted April 13, 1987.)

To facilitate the computation of the field scattered by a thin non-magnetic dielectric layer, it is customary to model the layer as an infinitesimally thin resitive sheet, but the simulation becomes increasingly inaccurate at oblique angles of incidence when the electric vector has a component normal to the layer. By starting with a volume integral formulation of the scattered field, it is shown that the accuracy is greatly improved when a "modified" conductive sheet is included in addition to the resistive one. The boundary conditions for the new sheet differ from those of a standard conductive sheet by the presence of a second normal derivative, and the combination of two coincident sheets yields results for a thin layer that are virtually indistinguishable from those provided by a volume integral equation. The advantages of this type of simulation are discussed, and the extension to a layer of arbitrary shape and composition is described.

1. INTRODUCTION

A common theme of several of Van Bladel's papers is the analysis and computation of the field scattered by a dielectric body, and this topic continues to be of interest. With the growing use of nonmetallic materials in man-made structures, a problem of particular concern is the modelling of a thin dielectric layer, possibly non-planar, in a manner that permits an accurate and efficient computation of the scattered field. For a nonmagnetic material a model that is widely used [*Harrington and Mautz*, 1975; *Senior*, 1979] is a resistive sheet, that is, an infinitesimally thin current sheet supporting an electric current proportional to the common value of the tangential electric field at its surfaces. The dual of this is a conductive sheet supporting only a magnetic current, and some of the properties of these sheets separately and in combination have been discussed by *Senior* [1985]. Under many circumstances a resistive sheet provides an effective simulation of a layer, but the accuracy decreases substantially at oblique angles of incidence when the electric vector has a component perpendicular to the layer. It is then necessary to supplement the model, and the way in which this can be done is the subject of the present paper.

Starting with a volume integral formulation of the scattering from a two-dimensional slab consisting of a homogeneous nonmagnetic material, it is shown (section 2) that coincident electric and magnetic current sheets provide an accurate simulation for all angles of incidence and polarization. The electric current satisfies the resistive sheet boundary conditions, while the magnetic current satisfies conditions which are similar to those for a conductive sheet but differ in the presence of a second normal derivative. The two sheets are decoupled when planar. As demonstrated in section 3, the combination of resistive and modified conductive sheets reproduces the known reflection coefficients for a thin layer of infinite extent, and computer codes based on this model yield results which are virtually identical to those produced by the volume integral formulation of *Richmond* [1965, 1966]. Some generalizations of the model are discussed in section 5, including the extension to a thin layer of arbitrary shape and composition. For such a layer the simulation consists of a pair of modified resistive and modified conductive sheets, and the resulting accuracy is significantly better than with the unmodified sheets.

Paper number 7S0490.
0048-6604/87/007S-0490$08.00

2. MATHEMATICAL DERIVATION

We consider the problem of a thin planar layer (or slab) consisting of a homogeneous nonmagnetic dielectric with relative permittivity (possibly complex) $\varepsilon = \varepsilon_1/\varepsilon_0$ illuminated by an electromagnetic field. The layer of thickness τ is centered on the plane $y = 0$,

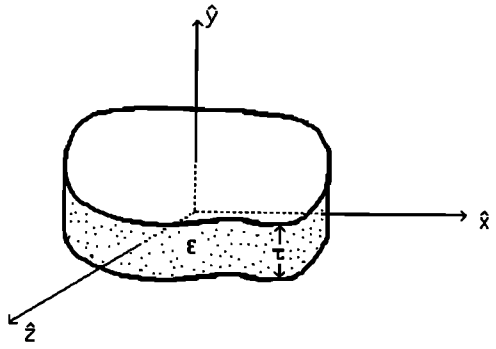

Fig. 1. Layer geometry.

and we seek to simulate the scattering using one or more infinitesimally thin sheets lying in this plane. The geometry is shown in Figure 1.

The scattered field can be attributed to a volume current density

$$\bar{J}^v = -ikY(\varepsilon - 1)\bar{E}^{\text{int}} \tag{1}$$

where $\bar{E}^{\text{int}}$ is the interior electric field, and $Y(= 1/Z)$ and k are the intrinsic admittance and propagation constant, respectively, of the surrounding free space medium. A time factor $e^{-i\omega t}$ has been assumed and suppressed. $\bar{J}^v$ is nonzero only within the volume V occupied by the layer, and since this is an electric current, the scattered field can be derived from the electric Hertz vector

$$\bar{\pi}(\bar{r}) = \frac{iZ}{k}\int_v \bar{J}^v(\bar{r}')G(\bar{r}, \bar{r}')dV' \tag{2}$$

where

$$G(\bar{r}, \bar{r}') = \frac{1}{4\pi}\frac{e^{ik|\bar{r}-\bar{r}'|}}{|\bar{r}-\bar{r}'|}$$

is the free space Green's function.

To a first approximation the net current flowing in the layer is

$$\bar{J}(x, z) = \frac{1}{2}\tau\left[\bar{J}^v\left(x, \frac{\tau}{2}, z\right) + \bar{J}^v\left(x, -\frac{\tau}{2}, z\right)\right]$$
$$= -\frac{i}{2}Yk\tau(\varepsilon - 1)\left[\bar{E}^{\text{int}}\left(x, \frac{\tau}{2}, z\right) + \bar{E}^{\text{int}}\left(x, -\frac{\tau}{2}, z\right)\right]$$

and when the continuity of the fields at $y = \pm\tau/2$ is enforced, we obtain

$$J_{x,z}(x, z) = -\frac{i}{2}Yk\tau(\varepsilon - 1)\left[E_{x,z}\left(x, \frac{\tau}{2}, z\right) + E_{x,z}\left(x, -\frac{\tau}{2}, z\right)\right]$$

$$J_y(x, z) = -\frac{i}{2}Yk\tau\frac{\varepsilon - 1}{\varepsilon}\left[E_y\left(x, \frac{\tau}{2}, z\right) + E_y\left(x, -\frac{\tau}{2}, z\right)\right]$$

which can be approximated by the following sheet currents in the plane $y = 0$:

$$J_{x,z}(x, z) = \frac{1}{2R}[E^+_{x,z} + E^-_{x,z}] \tag{3}$$

$$J_y(x, z) = \frac{Y^2}{2R^*_e}[E^+_y + E^-_y] \tag{4}$$

The plus and minus superscripts refer to the values of the exterior fields on the upper and lower surfaces of the sheet, respectively, and

$$R = \frac{iZ}{k\tau(\varepsilon - 1)} \tag{5}$$

$$R^*_e = \frac{iY\varepsilon}{k\tau(\varepsilon - 1)} \tag{6}$$

The currents defined in (3) and (4) constitute the sheet approximation to the dielectric layer, and the corresponding Hertz vector is

$$\bar{\pi}(\bar{r}) = \frac{iZ}{k}\int_S \bar{J}(x', z')G(\bar{r}, \bar{r}')\,dx'\,dz' \tag{7}$$

where S is the portion of the plane $y = 0$ occupied by the sheet.

To characterize the sheet we first consider the integral equations satisfied by the current components. The total electric field components are

$$E_x(\bar{r}) = E^i_x(\bar{r}) + \frac{iZ}{k}\int_S \left\{-J_x\left(\frac{\partial^2}{\partial y^2} + \frac{\partial^2}{\partial z^2}\right) + J_y\frac{\partial^2}{\partial x\partial y} + J_z\frac{\partial^2}{\partial x\partial z}\right\}G(\bar{r}, \bar{r}')\,dx'\,dz' \tag{8}$$

$$E_y(\bar{r}) = E^i_y(\bar{r}) + \frac{iZ}{k}\int_S \left\{J_x\frac{\partial^2}{\partial x\partial y} - J_y\left(\frac{\partial^2}{\partial x^2} + \frac{\partial^2}{\partial z^2}\right) + J_z\frac{\partial^2}{\partial y\partial z}\right\}G(\bar{r}, \bar{r}')\,dx'\,dz' \tag{9}$$

$$E_z(\bar{r}) = E^i_z(\bar{r}) + \frac{iZ}{k}\int_S \left\{J_x\frac{\partial^2}{\partial x\partial z} + J_y\frac{\partial^2}{\partial y\partial z} - J_z\left(\frac{\partial^2}{\partial x^2} + \frac{\partial^2}{\partial y^2}\right)\right\}G(\bar{r}, \bar{r}')\,dx'\,dz' \tag{10}$$

where the affix i denotes the incident field. From (8), on taking the limits as $\bar{r}$ approaches the sheet from above and below and adding, the terms which are odd functions of y cancel, giving

$$E^+_x + E^-_x = 2E^i_x + \left(\lim_{y\to 0+} + \lim_{y\to 0-}\right)\frac{iZ}{k}\int_S \left\{J_x\left(k^2 + \frac{\partial^2}{\partial x^2}\right) + J_z\frac{\partial^2}{\partial x\partial z}\right\}G(\bar{r}, \bar{r}')\,dx'\,dz'$$

and when the condition (3) is imposed, we then obtain

$$E_x^i(x, z) = RJ_x(x, z) - \lim_{y\to 0} \frac{iZ}{k} \int_S \left\{ J_x\left(k^2 + \frac{\partial^2}{\partial x^2}\right) + J_z \frac{\partial^2}{\partial x \partial z} \right\} G(\bar{r}, \bar{r}')\, dx'\, dz' \tag{11}$$

Similarly, from (10) and (3),

$$E_z^i(x, z) = RJ_z(x, z) - \lim_{y\to 0} \frac{iZ}{k} \int_S \left\{ J_x \frac{\partial^2}{\partial x \partial z} + J_z\left(k^2 + \frac{\partial^2}{\partial z^2}\right) \right\} G(\bar{r}, \bar{r}')\, dx'\, dz' \tag{12}$$

valid for a point on S, and (11) and (12) constitute the standard integral equations for a resistive sheet whose resistivity is R ohms per square.

This description of the sheet can be verified by examining the boundary conditions on S. From the expressions for the scattered magnetic field components it follows immediately that

$$H_x^+ - H_x^- = -J_z \qquad H_z^+ - H_z^- = J_x \tag{13}$$

and

$$H_y^+ = H_y^- \tag{14}$$

Hence, from (3),

$$E_x^+ + E_x^- = 2R[H_z^+ - H_z^-]$$

$$E_z^+ + E_z^- = -2R[H_x^+ - H_x^-]$$

which can be written more concisely as

$$\hat{y}x\{\hat{y}x[\bar{E}^+ + \bar{E}^-]\} = -2R\, \hat{y}\, x[\bar{H}^+ - \bar{H}^-] \tag{15}$$

The boundary conditions can also be expressed in terms of the field components normal to the layer. From Maxwell's equations in conjunction with (3),

$$H_y^+ + H_y^- = \frac{iY}{k}\left[\frac{\partial E_z^+}{\partial x} + \frac{\partial E_z^-}{\partial x} - \frac{\partial E_x^+}{\partial z} - \frac{\partial E_x^-}{\partial z}\right]$$

$$= -\frac{2iYR}{k}\left[\frac{\partial H_x^+}{\partial x} + \frac{\partial H_z^+}{\partial z} - \frac{\partial H_z^-}{\partial x} - \frac{\partial H_z^-}{\partial z}\right]$$

implying

$$H_y^+ + H_y^- + \frac{2R}{ikZ}\left[\frac{\partial H_y^+}{\partial y} - \frac{\partial H_y^-}{\partial y}\right] = 0 \tag{16}$$

Similarly,

$$\frac{\partial E_y^+}{\partial y} + \frac{\partial E_y^-}{\partial y} + \frac{2ikR}{Z}[E_y^+ - E_y^-] = 0 \tag{17}$$

and together with (14), these constitute alternative forms of the boundary conditions for a resistive sheet in the plane $y = 0$ [*Senior*, 1978].

In addition to J_x and J_z there is also a current component J_y, and from (9), by summing the limits as $\bar{r}$ approaches S from above and below,

$$E_y^+ + E_y^- = 2E_y^i + \left(\lim_{y\to 0+} + \lim_{y\to 0-}\right)\frac{iZ}{k}\left(k^2 + \frac{\partial^2}{\partial y^2}\right) \cdot \int_S J_y\, G(\bar{r}, \bar{r}')\, dx'\, dz'$$

leading to the integral equation

$$E_y^i(x, z) = Z^2 R_e^*\, J_y(x, z) - \lim_{y\to 0} ikZ\left(1 + \frac{1}{k^2}\frac{\partial^2}{\partial y^2}\right) \cdot \int_S J_y\, G(\bar{r}, \bar{r}')\, dx'\, dz' \tag{18}$$

The corresponding sheet is coincident with the resistive one and consists of a layer of electric dipoles oriented perpendicular to the plane $y = 0$. Alternatively, since

$$J_y = \frac{iY}{k}\, \hat{y} \cdot \nabla x \bar{J}^*,$$

the field can be attributed to a magnetic current $\bar{J}^*$ in the plane $y = 0$. Equation (18) is, in fact, the integral equation for a conductive sheet [*Senior*, 1985] modified by the presence of the derivative on the right-hand side, and this description of the sheet is confirmed by the boundary conditions.

From (9) by first differentiating with respect to y and then subtracting the limits as $\bar{r}$ approaches S from above and below,

$$\frac{\partial E_y^+}{\partial y} - \frac{\partial E_y^-}{\partial y} = -ik\, Z\left(1 + \frac{1}{k^2}\frac{\partial^2}{\partial y^2}\right)J_y$$

[*Van Bladel*, 1985], and (4) now gives

$$\left(1 + \frac{1}{k^2}\frac{\partial^2}{\partial y^2}\right)(E_y^+ + E_y^-) + \frac{2R_e^*}{ikY}\left[\frac{\partial E_y^+}{\partial y} - \frac{\partial E_y^-}{\partial y}\right] = 0 \tag{19}$$

Apart from the second derivative, this is identical to the boundary condition for a conductive sheet of conductivity R_e^* mhos per square supporting a magnetic current

$$J_z^* = E_x^+ - E_x^-$$

Just as the resistive sheet conditions (16) and (17) admit a single vector expression involving the

tangential field components, so too does (19). From (8), (4) and Maxwell's equations,

$$E_x^+ - E_x^- = -\frac{iZ}{k}\frac{\partial J_y}{\partial x} = -\frac{iY}{2kR_e^*}\left[\frac{\partial E_y^+}{\partial x} + \frac{\partial E_y^-}{\partial x}\right]$$

giving

$$E_x^+ - E_x^- = \frac{1}{2R_e^*}[H_z^+ + H_z^-] - \frac{iY}{2kR_e^*}\left[\frac{\partial E_x^+}{\partial y} + \frac{\partial E_x^-}{\partial y}\right]$$

Similarly,

$$E_z^+ - E_z^- = -\frac{1}{2R_e^*}[H_x^+ + H_x^-] - \frac{iY}{2kR_e^*}\left[\frac{\partial E_z^+}{\partial y} + \frac{\partial E_z^-}{\partial y}\right]$$

and these can be written more concisely as

$$\hat{y}x\{\hat{y}x[\bar{H}^+ + \bar{H}^-]\} = 2R_e^*\,\hat{y}x[\bar{E}^+ - \bar{E}^-] + \frac{iY}{k}\,\hat{y}x\frac{\partial}{\partial y}[\bar{E}^+ + \bar{E}^-] \tag{20}$$

It can be verified that this implies (14).

The layer simulation that has been developed consists of coincident resistive and modified conductive sheets. The boundary conditions can be written as (15) and (20) or (14), (16), (17) and (19), where R and R_e^* are defined in (5) and (6), respectively, and for a planar layer the two sets are equivalent. The individual sheets are uncoupled when planar. As shown later, the inclusion of the modified conductive sheet in addition to the resistive one is necessary to provide a good simulation at oblique incidence when the incident electric vector has a component perpendicular to the layer.

A special case of importance for the sequel is a dielectric slab illuminated by a plane wave incident in the xy plane. This is a two-dimensional problem in which there is no dependence on the z coordinate, and it is convenient to consider separately two types of illumination: (1) E polarization for which the electric vector is perpendicular to the plane of incidence so that $E_y = 0$; and (2) H polarization for which the electric vector is in the plane of incidence, implying $H_y = 0$. For E polarization the boundary conditions expressed in terms of the normal field component H_y are (14) and (16). The resistive sheet alone is excited, and since the only nonzero current component is J_z, the required integral equation is (see 12)

$$E_z^i(x) = RJ_z(x) + \frac{kZ}{4}\int_l J_z(x')H_0^{(1)}(k|x - x'|)\,dx' \tag{21}$$

where l is the lateral extent of the sheet in the plane $y = 0$ and $H_0^{(1)}$ is the Hankel function of the first kind of order zero. For H polarization the corresponding boundary conditions are (17) and (19). Both sheets are now excited, and the relevant integral equations are (see 11 and 18)

$$E_x^i(x) = RJ_x(x) - \lim_{y\to 0}\frac{Z}{4k}\frac{\partial^2}{\partial y^2}\int_l \cdot J_x(x')H_0^{(1)}(k\sqrt{(x - x')^2 + y^2})\,dx' \tag{22}$$

and

$$E_y^i(x) = Z^2R_e^*J_y(x) + \lim_{y\to 0}\frac{kZ}{4}\left(1 + \frac{1}{k^2}\frac{\partial^2}{\partial y^2}\right)\int_l \cdot J_y(x')H_0^{(1)}(k\sqrt{(x - x')^2 + y^2})\,dx' \tag{23}$$

Apart from the derivative term in (23), these are the standard integral equations for resistive and conductive sheets.

3. FRESNEL REFLECTION COEFFICIENTS

A limiting case of a finite layer is a layer of infinite extent, and if the layer simulation is to be effective, it must also be accurate in this case. To verify this, we compare the Fresnel reflection coefficients for a plane wave having

$$H_y(E_y) = e^{ik(x\cos\phi_0 - y\sin\phi_0)}$$

corresponding to $E(H)$ polarization, incident on a layer occupying $-\infty < x,\ z < \infty,\ -\tau/2 < y < \tau/2$ with the reflection coefficients provided by our simulations.

The Fresnel reflection coefficients for the layer are

$$\Gamma = \mp e^{ik\tau\sin\phi_0}\left\{1 + \frac{2}{\gamma^2 - 1} \cdot [1 + i\gamma\cot(k\tau\sqrt{\varepsilon - \cos^2\phi_0})]\right\}^{-1} \tag{24}$$

with the upper (lower) sign for $E(H)$ polarization and

$$\gamma = \frac{\sqrt{\varepsilon - \cos^2\phi_0}}{\sin\phi_0} \qquad E \text{ polarization}$$

$$\gamma = \frac{\varepsilon\sin\phi_0}{\sqrt{\varepsilon - \cos^2\phi_0}} \qquad H \text{ polarization}$$

Assuming $|\,k\tau(\varepsilon - \cos^2\phi_0)^{1/2}\,|$ is small, so that

$$\cot(k\tau\sqrt{\varepsilon - \cos^2\phi_0}) \simeq (k\tau\sqrt{\varepsilon - \cos^2\phi_0})^{-1}$$

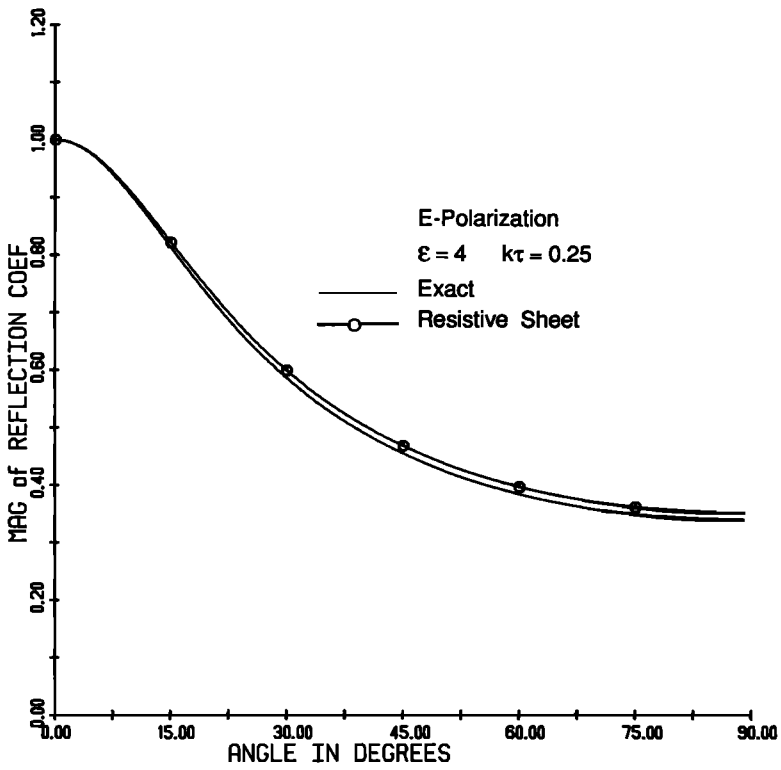

Fig. 2. Magnitude of the reflection coefficient for a planar layer with $k\tau = 0.25$ and $\varepsilon = 4$; E polarization.

the reflection coefficients can be approximated as

$$\Gamma_E = -e^{-ik\tau \sin \phi_0} \left\{1 + \frac{2 \sin \phi_0}{\varepsilon - 1} \left(\sin \phi_0 + \frac{i}{k\tau}\right)\right\}^{-1} \tag{25}$$

and

$$\Gamma_H = e^{-ik\tau \sin \phi_0} \left\{1 + \frac{2}{(\varepsilon - 1)(\varepsilon \sin^2 \phi_0 - \cos^2 \phi_0)} \cdot \left(\varepsilon - \cos^2 \phi_0 + \frac{i\varepsilon \sin \phi_0}{k\tau}\right)\right\}^{-1} \tag{26}$$

for E and H polarizations, respectively. To a good approximation,

$$\Gamma_E \approx -\left\{1 + \frac{2i \sin \phi_0}{k\tau(\varepsilon - 1)}\right\}^{-1} \tag{27}$$

but because of the Brewster angle occurring at $\phi_0 = \cot^{-1} \varepsilon^{1/2}$, there is no similar approximation to Γ_H that is valid for all angles.

For a resistive sheet with E polarization

$$\Gamma_E = -\left\{1 + \frac{2R}{Z} \sin \phi_0\right\}^{-1} \tag{28}$$

and this is identical to (27) when R has the value given in (5). For H polarization, the resistive and modified conductive sheets give

$$\begin{aligned}\Gamma_H &= \left\{1 + \frac{2R}{Z \sin \phi_0}\right\}^{-1} - \left\{1 + \frac{2R_c^*}{Y} \frac{\sin \phi_0}{\cos^2 \phi_0}\right\}^{-1} \\ &= \left\{1 + \frac{2i}{k\tau(\varepsilon - 1) \sin \phi_0}\right\}^{-1} \\ &\quad - \left\{1 + \frac{2i\varepsilon \sin \phi_0}{k\tau(\varepsilon - 1) \cos^2 \phi_0}\right\}^{-1}\end{aligned} \tag{29}$$

and this displays the Brewster angle phenomenon. As expected, the two sheets scatter independently, and the reflection coefficient is the sum of the reflection coefficients of the sheets in isolation.

In Figures 2–9 the amplitudes and phases of the exact reflection coefficients (24) are compared with those provided by the sheet simulations. Overall the agreement is good, and the inclusion of the conductive sheet produces a significant improvement for H polarization, particularly at the wider angles. The phase discrepancy which is evident for ϕ_0 near $\pi/2$ is almost entirely due to the multiplicative phase factor

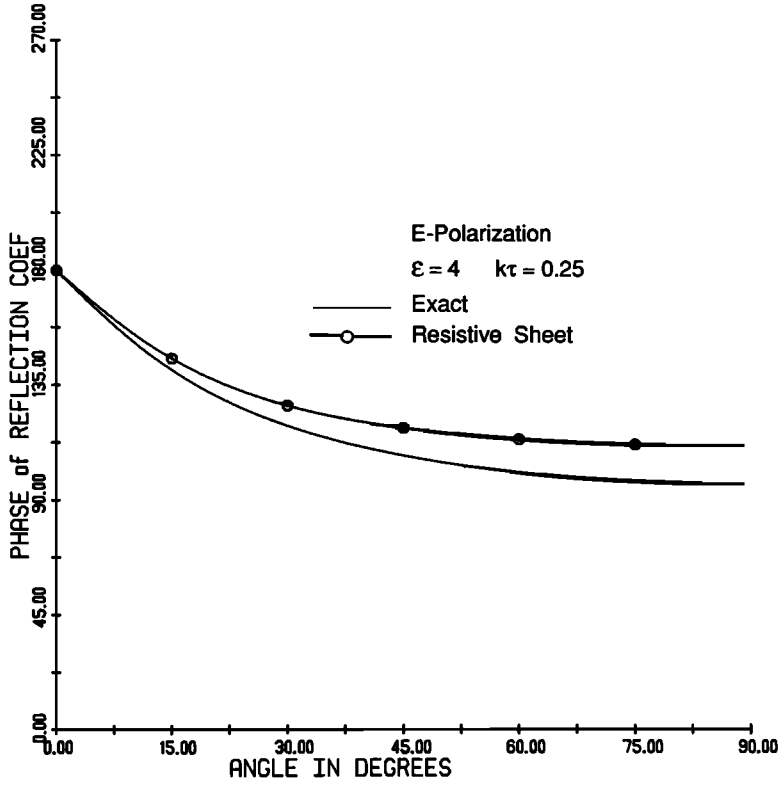

Fig. 3. Phase of the reflection coefficient for a planar layer with $k\tau = 0.25$ and $\varepsilon = 4$; E polarization.

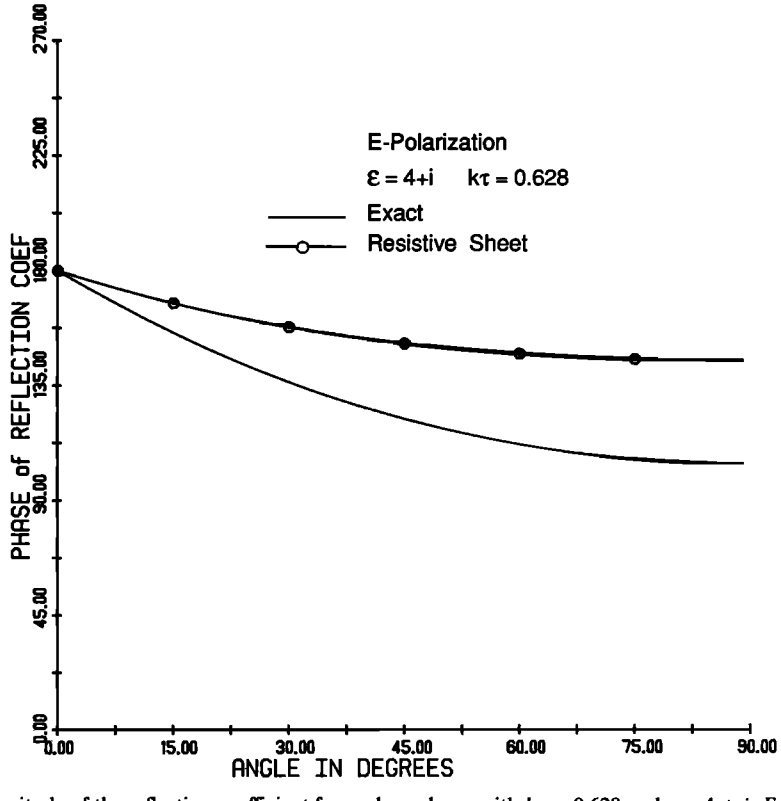

Fig. 4. Magnitude of the reflection coefficient for a planar layer with $k\tau = 0.628$ and $\varepsilon = 4 + i$; E polarization.

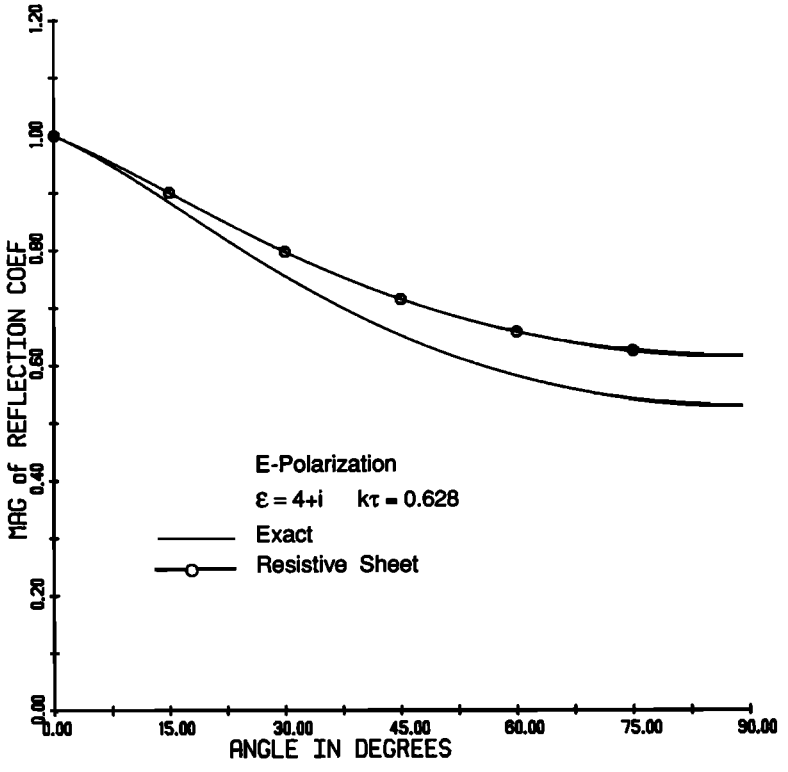

Fig. 5. Phase of the reflection coefficient for a planar layer with $k\tau = 0.628$ and $\varepsilon = 4 + i$; E polarization.

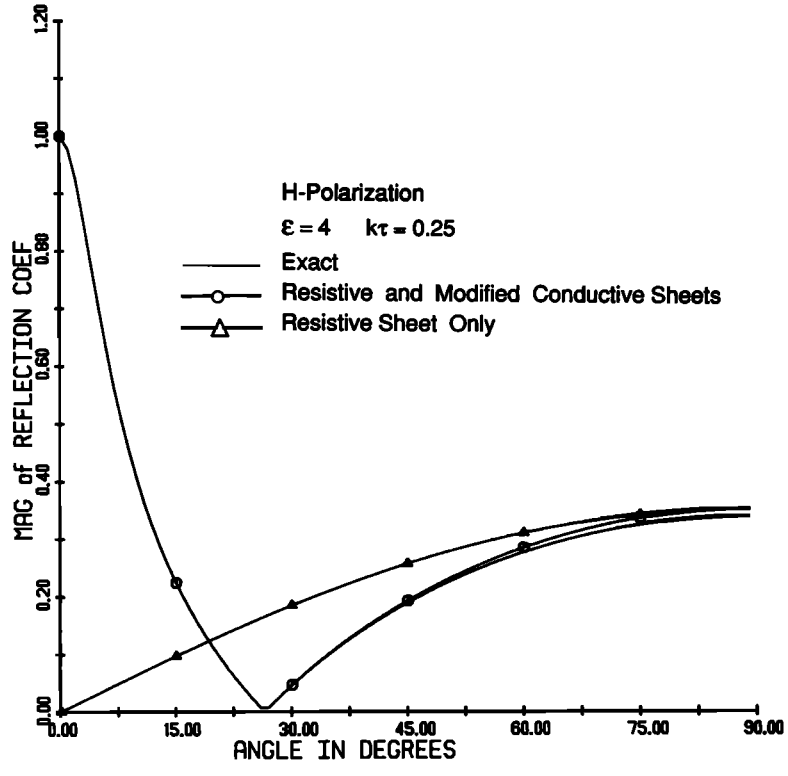

Fig. 6. Magnitude of the reflection coefficient for a planar layer with $k\tau = 0.25$ and $\varepsilon = 4$; H polarization.

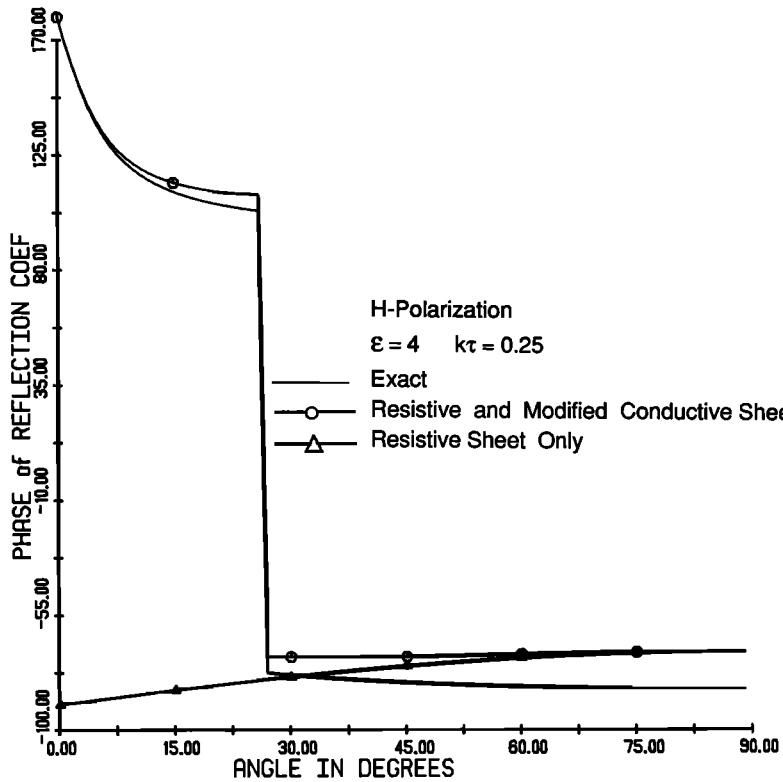

Fig. 7. Phase of the reflection coefficient for a planar layer with $k\tau = 0.25$ and $\varepsilon = 4$; H polarization.

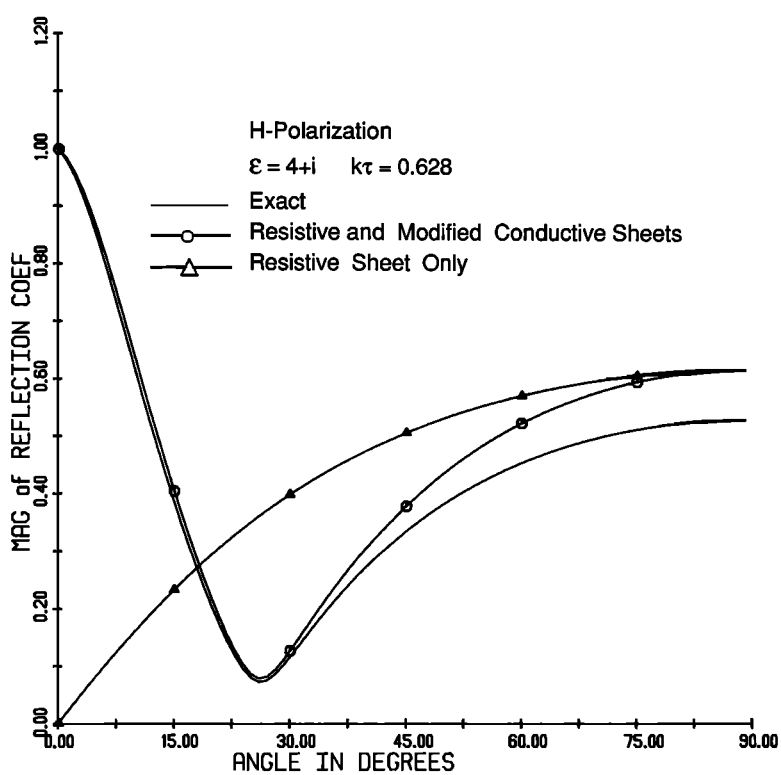

Fig. 8. Magnitude of the reflection coefficient for a planar layer with $k\tau = 0.628$ and $\varepsilon = 4 + i$; H polarization.

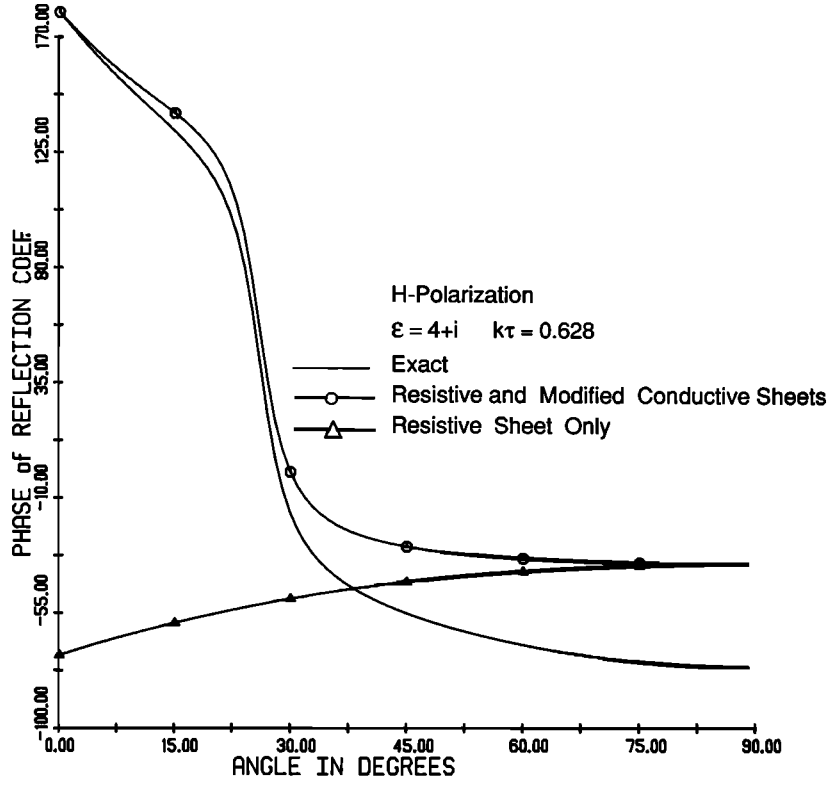

Fig. 9. Phase of the reflection coefficient for a planar layer with $k\tau = 0.628$ and $\varepsilon = 4 + i$; H polarization.

in (24), and is eliminated if the sheets are placed at the upper surface of the layer rather than the middle.

4. THEORETICAL AND NUMERICAL COMPARISONS

In the previous section it was shown that for both polarizations the sheet boundary conditions (15) and (20) or, equivalently, (14), (16), (17) and (19), provide a close approximation to the reflection coefficients of a thin layer. In addition, for H polarization *Leppington* [1983] developed a pair of boundary conditions to simulate the effect of traveling waves on a thin slab of infinite extent, and though the derivation differs from that which we employed, the boundary conditions are identical to (17) and (19). Nevertheless, for a complete test of the sheet simulation, it is necessary to consider a finite slab and to compare the far fields obtained using (15)–(20) with those found by (say) solving the volume integral equations.

Solutions of the volume integral equations for two-dimensional (cylindrical) dielectrics have been developed by *Richmond* [1965, 1966] for E and H polarizations. Using the method of moments, the dielectric is subdivided into rectangular cells (or cylinders) with the volume electric current density $\bar{J}^v$ assumed constant over each, thereby converting the integral equation into a matrix equation for the sampled current values. By replacing the cells with equivalent circular ones, the integrations over the cells can be carried out analytically. A thin dielectric slab can be subdivided into one or more rows of cells, and for the slab thicknesses considered here, it was found that a single row suffices. We now compare the resulting integral equations and the scattered field produced with those based on the sheet simulation.

4.1. *E polarization*

With this polarization the modified conductive sheet is not excited and the resistive sheet alone is present. The integral equation implied by (15) is (21), whose numerical solution can be found by subdividing l into segments of length δ with J_z assumed constant over each. This leads to the system of equations

$$\sum_n A_{mn} J_{zn} = E^i_{zm} \tag{30}$$

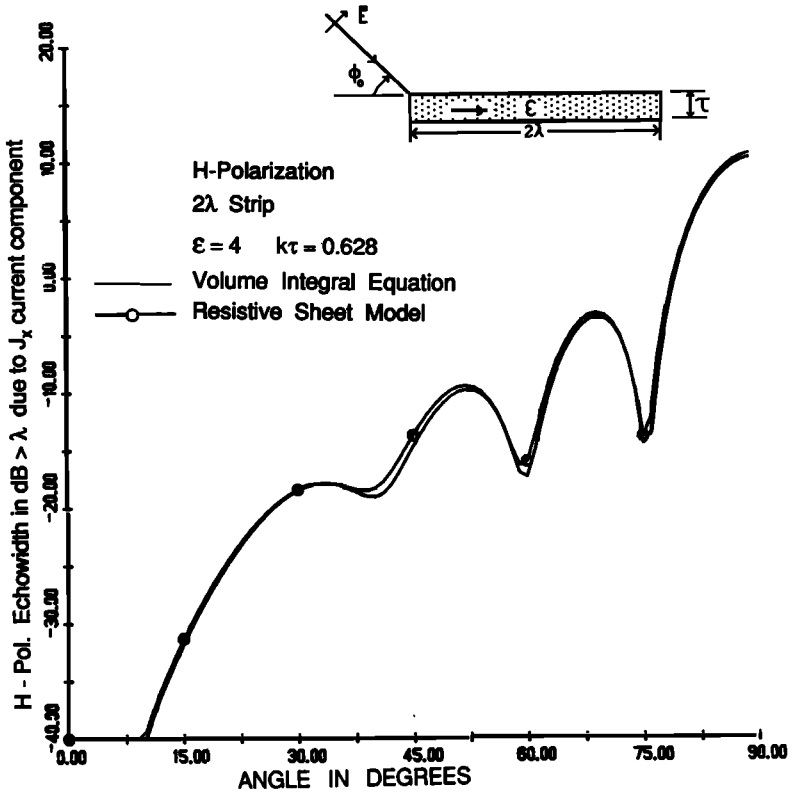

Fig. 10. Comparison of the H-polarized backscattered field contributed by the tangential current component (J_x) with that of the resistive sheet model for a 2λ-wide slab having $k\tau = 0.628$ and $\varepsilon = 4$.

with

$$A_{mn} = Z\frac{k\delta}{4}H_0^{(1)}(k|x_m - x_n|) \tag{31}$$

for $m \neq n$ and

$$A_{nn} = R + Z\frac{k\delta}{4}\left\{1 + \frac{2i}{\pi}\left[ln\frac{k\delta}{4} - 0.4222\right]\right\} \tag{32}$$

where E_{zm}^i are the incident field values at $x = x_m$ on $y = 0$ and J_{zn} are the sampled values of the sheet current.

The scattered field produced by this current is identical to that obtained using *Richmond*'s [1965] formulation, and the reason becomes obvious when we compare the matrix elements. Inherent in Richmond's formulation is the approximation

$$\bar{J}(x) = \frac{1}{2R}\left\{\bar{E}^{int}\left(x, \frac{\tau}{2}\right) + \bar{E}^{int}\left(x, -\frac{\tau}{2}\right)\right\} \simeq \frac{1}{R}\bar{E}^{int}(x, 0)$$

With this substitution in (30), the A_{mn}/R are identical to Richmond's matrix elements provided the Bessel function $J_1(ka)$ is approximated as $ka/2$, where $a = \tau/(\pi)^{1/2}$ is the radius of the equivalent circular cell and our solution is specialized by taking $\delta = \tau$.

4.2. *H polarizaton*

In contrast to the previous case, the modified conductive sheet is now excited. Both sheets are necessary to accurately simulate a thin dielectric slab, and the integral equations implied by the boundary conditions (15) and (20) are (22) and (23). These can be discretized as

$$\begin{aligned}\sum_n B_{mn} J_{xn} &= E_{xm}^i \\ \sum_n C_{mn} J_{yn} &= E_{ym}^i\end{aligned} \tag{33}$$

and by employing the relation $\partial^2/\partial y^2 = -(k^2 + \partial^2/\partial x^2)$, the integrations over the cells can be carried out to give [*Peters et al.*, 1986]

$$B_{mn} = Z\frac{k\delta}{4}\frac{H_1^{(1)}(k|x_m - x_n|)}{|x_m - x_n|} \tag{34}$$

$$C_{mn} = \frac{k\delta}{4}Z\left\{kH_0^{(1)}(k|x_m - x_n|) - \frac{H_1^{(1)}(k|x_m - x_n|)}{|x_m - x_n|}\right\} \tag{35}$$

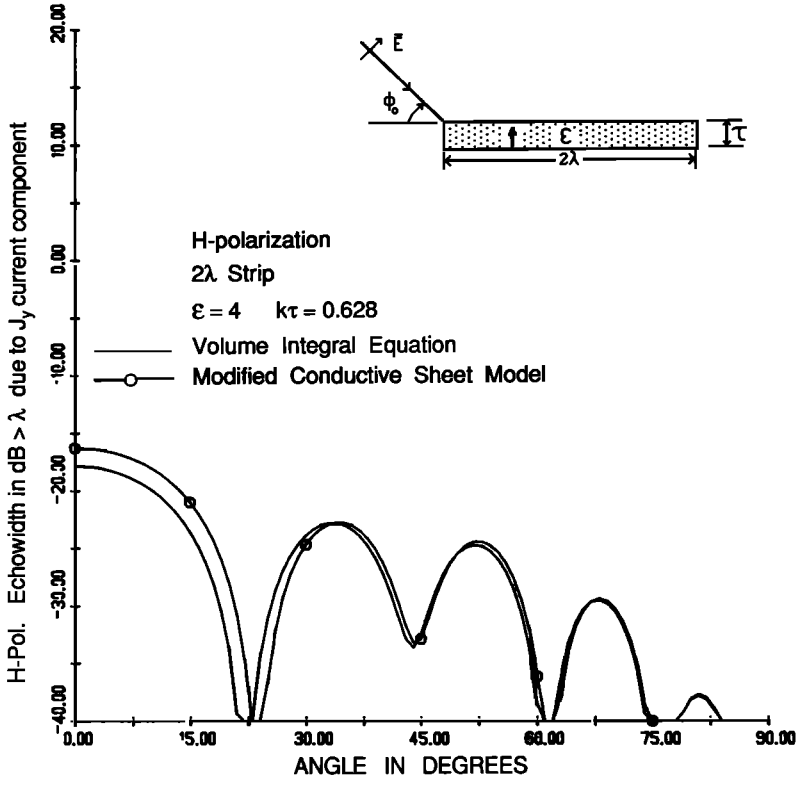

Fig. 11. Comparison of the H-polarized backscattered field contributed by the normal current component (J_y) with that of the modified conductive sheet for a 2λ wide slab having $k\tau = 0.628$ and $\varepsilon = 4$.

for $m \neq n$, and

$$B_{nn} = C_{nn} = R + Z\frac{k\delta}{8}\left\{1 + \frac{2i}{\pi}\left[\frac{8}{(k\delta)^2} + ln\frac{k\delta}{4} - 0.9228\right]\right\} \tag{36}$$

The amplitudes of the far zone scattered fields generated by the individual current components in (33) are plotted in Figures 10 and 11 for a 2λ-wide slab having $\varepsilon = 4$ and $\tau = \lambda/10$. The conductive sheet accounts for the traveling wave effects at near-grazing angles of incidence, and the complete scattered field is the sum of the two contributions. As seen from the plots, the sheets produce results which are very close to those obtained from *Richmond*'s [1966] formulation, thereby confirming the validity of the sheet simulation. Indeed, under the same approximations discussed in connection with E polarization, the matrix elements B_{nm} and C_{mn} are identical to Richmond's.

5. CONCLUDING REMARKS

We have shown that a thin nonmagnetic dielectric slab can be simulated with a pair of coincident resistive and modified conductive sheets satisfying the boundary conditions (15) and (20), respectively. The sheets are uncoupled when planar and the resulting integral equations are numerically equivalent to those developed by *Richmond* [1965, 1966] based on a volume integral formulation. For a thicker slab it is natural to consider a stack of these sheets, and *Peters et al.* [1986] have shown that a slab of arbitrary thickness can be modelled in this way, but for a thick dielectric of general shape it is more convenient to employ nonplanar sheets. The corresponding boundary conditions can be deduced from (15) and (20) by replacing y by the normal distance n, where $\hat{n}$ is the unit vector normal drawn outwards from the positive side of the sheet, giving

$$\hat{n}x\{\hat{n}x[\bar{E}^+ + \bar{E}^-]\} = -2R\hat{n}x[\bar{H}^+ - \bar{H}^-] \tag{37}$$

$$\hat{n}x\{\hat{n}x[\bar{H}^+ + \bar{H}^-]\} - \frac{iY}{k}\hat{n}x\frac{\partial}{\partial n}[\bar{E}^+ + \bar{E}^-]$$

$$= 2R_c^*\,\hat{n}x[\bar{E}^+ - \bar{E}^-] \tag{38}$$

By invoking duality we can also specify the sheets required to simulate a thin layer of magnetic ($\mu \neq 1$) material whose relative permittivity is unity. The

sheets are conductive and modified resistive ones satisfying the boundary conditions

$$\hat{n}x\{\hat{n}x[\bar{H}^+ + \bar{H}^-]\} = 2R^*\hat{n}x[\bar{E}^+ - \bar{E}^-] \tag{39}$$

$$\hat{n}x\{\hat{n}x[\bar{E}^+ + \bar{E}^-]\} + \frac{iZ}{k}\hat{n}x\frac{\partial}{\partial n}[\bar{H}^+ + \bar{H}^-]$$

$$= -2R_m\hat{n}x[\bar{H}^+ - \bar{H}^-] \tag{40}$$

with

$$R^* = \frac{iY}{k\tau(\mu - 1)} \tag{41}$$

$$R_m = \frac{iZ\mu}{k\tau(\mu - 1)} \tag{42}$$

More generally, for a layer of material whose permittivity and permeability are both arbitrary, the boundary conditions are

$$\hat{n}x\left\{\hat{n}x\left(\frac{1}{2R} + \frac{1}{2R_m}\right)[\bar{E}^+ + \bar{E}^-]\right\}$$

$$+ \frac{iZ}{2kR_m}\hat{n}x\frac{\partial}{\partial n}[\bar{H}^+ + \bar{H}^-] = -\hat{n}x[\bar{H}^+ - \bar{H}^-] \tag{43}$$

$$\hat{n}x\left\{\hat{n}x\left(\frac{1}{2R^*} + \frac{1}{2R_e^*}\right)[\bar{H}^+ + \bar{H}^-]\right\}$$

$$- \frac{iY}{2kR_e^*}\hat{n}x\frac{\partial}{\partial n}[\bar{E}^+ + \bar{E}^-] = \hat{n}x[\bar{E}^+ - \bar{E}^-] \tag{44}$$

defining a pair of modified resistive and modified conductive sheets, where R, R_e^*, R^* and R_m are given in (5), (6), (41) and (42), respectively.

In the particular case of planar sheets lying in the plane $y = 0$, (43) and (44) are equivalent to the scalar boundary conditions

$$\frac{\partial E_y^+}{\partial y} + \frac{\partial E_y^-}{\partial y} + \frac{2ikR}{Z}[E_y^+ - E_y^-] = 0 \tag{45}$$

$$\left\{\frac{1}{2R^*} + \frac{1}{2R_e^*}\left(1 + \frac{1}{k^2}\frac{\partial^2}{\partial y^2}\right)\right\}[E_y^+ + E_y^-]$$

$$+ \frac{Z}{ik}\left[\frac{\partial E_y^+}{\partial y} - \frac{\partial E_y^-}{\partial y}\right] = 0 \tag{46}$$

$$\frac{\partial H_y^+}{\partial y} + \frac{\partial H_y^-}{\partial y} + \frac{2ikR^*}{Y}[H_y^+ - H_y^-] = 0 \tag{47}$$

$$\left\{\frac{1}{2R} + \frac{1}{2R_m}\left(1 + \frac{1}{k^2}\frac{\partial^2}{\partial y^2}\right)\right\}[H_y^+ + H_y^-]$$

$$+ \frac{Y}{ik}\left[\frac{\partial H_y^+}{\partial y} - \frac{\partial H_y^-}{\partial y}\right] = 0 \tag{48}$$

These are examples of generalized boundary conditions similar to those proposed by *Karp and Karal* [1965] in which higher order normal derivatives were introduced to more accurately simulate a desired angular dependence of the reflection coefficient of a surface. In principle at least, an advantage of this type of generalization is that the boundary condition still permits the analytical solution of the corresponding half plane problem using the Wiener-Hopf technique, enabling the edge diffracted field to be determined (see, for example, *Chakrabarti* [1986]).

Acknowledgments. This work was supported in part by the U.S. Army under contract DAAA 15-86-K-0022 and by Rockwell International–NAAO under purchase order L6XN-395803-913.

REFERENCES

Chakrabarti, A., Diffraction by a dielectric half plane, *IEEE Trans. Antennas Propag., AP-34*, 830–833, 1986.

Harrington, R. F., and J. R. Mautz, An impedance sheet approximation for thin dielectric shells, *IEEE Trans. Antennas Propag., AP-23*, 531–534, 1975.

Karp, S. N., and F. C. Karal, Jr., Generalized impedance boundary conditions with applications to surface wave structures, in *Electromagnetic Wave Theory, Part 1*, edited by J. Brown, pp. 479–483, Pergamon, New York, 1965.

Leppington, F. G., Travelling waves in a dielectric slab with an abrupt change in thickness, *Proc. R. Soc. London, Ser. A, 386*, 443–460, 1983.

Peters, T. J., J. L. Volakis, V. V. Liepa, T. B. A. Senior, and M. A. Ricoy, Simulation of two-dimensional dielectric structures with resistive sheets, *Rep. 389055-1-F*, Univ. of Mich. Radiat. Lab., Ann Arbor, Mich., 1986.

Richmond, J. H., Scattering by a dielectric cylinder of arbitrary cross-section shape, *IEEE Trans. Antennas Propag., AP-13*, 334–341, 1965.

Richmond, J. H., TE-wave scattering by a dielectric cylinder of arbitrary cross-section shape, *IEEE Trans. Antennas Propag., AP-14*, 460–464, 1966.

Senior, T. B. A., Some problems involving imperfect half planes, in *Electromagnetic Scattering*, edited by P. L. E. Uslenghi, pp. 185–219, Academic, Orlando, Fla., 1978.

Senior, T. B. A., Backscattering from resistive strips, IEEE Trans. Antennas Propag., *AP-27*, 808–813, 1979.

Senior, T. B. A., Combined resistive and conductive sheets, *IEEE Trans. Antennas Propag., AP-33*, 577–579, 1985.

Van Bladel, J., *Electromagnetic Fields*, p. 354, Hemisphere, New York, 1985.

T. B. A. Senior and J. L. Volakis, Radiation Laboratory, Department of Electrical Engineering and Computer Science, University of Michigan, Ann Arbor, MI 48109.